EDGE DIFFRACTION IN ROOM ACOUSTICS COMPUTATIONS

PACS REFERENCE: 43.55.Ka

Torres, Rendell R. [1]; Svensson, U. Peter [2]; Kleiner, Mendel [1]
1 Chalmers Room Acoustics Group. Department of Applied Acoustics
Chalmers University of Technology
SE-412 96 Gothenburg. Sweden;
Tel: 46 317 722 210. Fax: 46 317 722 212
E-mail: rendell@ta.chalmers.se
2 Acoustics Group. Department of Telecommunications, NTNU
NO-7491 Trondheim Norway
Tel: 47735 90 546. Fax: 47 735 91 412
E-mail: svensson@tele.ntnu.no

ABSTRACT

Computation and auralization of room impulse responses currently lack a sufficient treatment of edge diffraction, i.e., the scattering from edges of finite surfaces. A validated time-domain model has been applied to two cases: (1) a conservative stage-house geometry (with large, smooth surfaces) where low-frequency diffraction was still audible for certain input signals, and (2) a smaller reflector array, where the edge diffraction affects higher frequencies. Computational considerations such as edge-visibility checks and binaural implementation are also discussed.

INTRODUCTION

Computation and auralization of room impulse responses (RIR) is commonly done using geometrical-acoustics models with Lambert-diffusion approximations to simulate non-specular scattering. Edge diffraction, however, is a fundamental component of the sound field around any finite reflecting surface. In room acoustics, for example, it describes not only the commonly noted phenomenon of sound propagating around corners (or emitting from orchestra pits) but also the scattering in *all* directions from wedges of any angle, e.g., the finite walls of a stage-house proscenium or the “knife-edges” of thin overhead reflectors. For frequencies low enough that small-scale surface scattering becomes negligible, one may even consider much of a room’s interior as a simple assemblage of various wedges that reflect and diffract.

Edge diffraction is computed here using a time-domain, finite-edge version of the exact Biot-Tolstoy solution [1], developed first by Medwin *et al*. [9,10] (and often called the BTM model) and further by Svensson *et al*. [12]. Svensson *et al.* derived analytical directivity functions for the edge sources (see Fig. 1a), which justified Medwin’s assumptions for modeling first-order diffraction and refined the BTM modeling of second-order diffraction, which becomes more important for grazing angles and decreasing surface dimensions [5]. This diffraction model thus yields diffraction impulse responses (compatible with image source approaches and suitable for auralization) and does not rely on the Kirchhoff Approximation, which fails for diffraction calculations not only at "lower" frequencies but at *all* frequencies for certain angles of incidence [3, 10]. The analytical expressions and calculation method are given in Ref. 12 (Eqs. 12, 19, 28-29, and Sec. II) and excluded here for brevity.

Figure 1(a) schematically depicts the analytical model. For reflection from an infinite rigid plane, the conventional image source model is an exact “equivalent source.” A change of impedance on the plane (i.e., at the edges of a finite reflector) results in scattering (modeled by edge sources) which interferes with the specular reflection (i.e., the image source *S¢*). Note that

energy-based Lambert "diffusion" methods neglect phase information and inherently cannot replicate the correct interference effects of edge diffraction components from non-specular directions to the receiver [13]. Furthermore, even if some phase is assumed, a Lambert edge source directs its lobe maximum in the normal direction from the plane and does not reproduce the actual, more complex (diffraction) directivity, which varies with incidence angle and position along the edge.

The model has been validated for several different geometries, such as a circular disc and a thin rectangular plate [5,12], a right-angle step discontinuity [2], thick barriers [10, 16], double-diffraction from knife-edges [16], and 2D "wedge assemblages" of spheres and rough surfaces [6, 7]. The individual "wedges" for the examples below fall within these cases, so we concentrate here primarily on applying the computations to room acoustics.

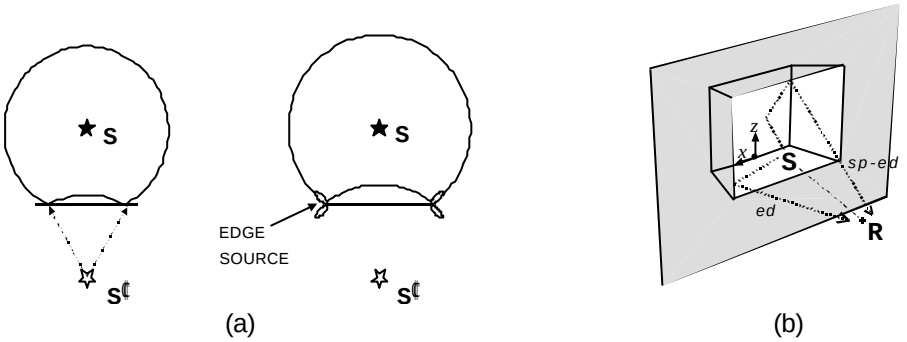

Figure 1. (a) Schematic drawing of edge sources, (b) stage-house example.

A CONSERVATIVE TEST GEOMETRY

The analytical model by Svensson *et al*. was initially applied in room acoustics to calculating diffraction from the edges of an unenclosed stage-house [14] shown in Figure 1(b). (Ouis [11] and Kovitz [8], however, have applied the BT solution in simpler forms.) The proscenium height and width are 14.5 m and 18.6 m. The back wall is 12.5 m high and 14 m wide. The stage depth is 8.3 m, with a horizontal floor. The stage-house sits eccentrically (Δx = -0.8 m, Δz = 1.25) in the finite baffle, with height 30 m and width 40 m. With the origin bisecting the rear-floor edge, the source's and receiver's coordinates are (-2, 7, 1.18) and (-2, 20.9, -0.4) [m].

The stage-house form was chosen as an ideal conservative test geometry. First, it is a "typical" concert hall component with a complex shape involving several different wedge angles and many different reflection-diffraction paths. It is also a "conservative" geometry where geometrical acoustics should hold for most reflection paths (except at very low frequencies), due to the large dimensions of the smooth reflecting surfaces. The "non-shadowed" source-receiver orientation was also conservative, compared to receiver positions hidden from the source. The computations employed edge-visibility checks (described below) to include combinations of specular/diffractive components, e.g., the path *sp-ed* (*specular* reflection to *edge* diffraction) in Figure 1(b). Such paths greatly improved agreement between computed RIR and scale-model measurements, and the total contribution from edge diffraction (first- and second-order direct paths, plus *sp-ed*, *ed-sp*, and *sp-ed-sp*) are shown in solid lines in Figure 2(a). Moreover, without these extra combinations, the total edge diffraction would be incompletely predicted.

In the frequency-response function in Fig. 2(b) for the RIR "with and without" the total computed diffraction, level differences of only about 1-2 dB appeared below about 200 Hz. Nevertheless, "ABX" listening tests showed that this small spectral change was clearly audible for certain input signals. Here the impulse responses with different orders and components of diffraction were convolved with the following anechoic signals: pink noise, (synthesized) organ music, male and female speech, and an impulse (which, one may note, emphasizes effects at higher frequencies). The test taker specified whether a given sound "X" was the same as sound "A" or "B" where, for example, "A" was an RIR with diffraction and "B" was one without diffraction. For this study, a significance level of $P(r)$ < 5% (binomial distribution) was utilized. Thus, with 18 subjects, a ratio of 13 correct answers of 18 ($P(r)$ = 3.3%) gave the threshold for a significant audible difference. Cases where 11-12 correct answers were given ($P(r)$ = 7–12 %) were marginally

significant and called “possibly audible.” The question “Are the diffraction contributions audible?” corresponded to ABX pairs with or without the total computed diffraction. The question “Is second-order diffraction audible?” corresponded to ABX pairs with or without second-order diffraction. (Such questions, of course, were not posed to the test takers.) Some initial results are shown in the table below, where the parentheses contain ratios of correct answers. (These results were obtained after computational corrections that revealed greater diffraction effects than described in previously published proceedings [14].)

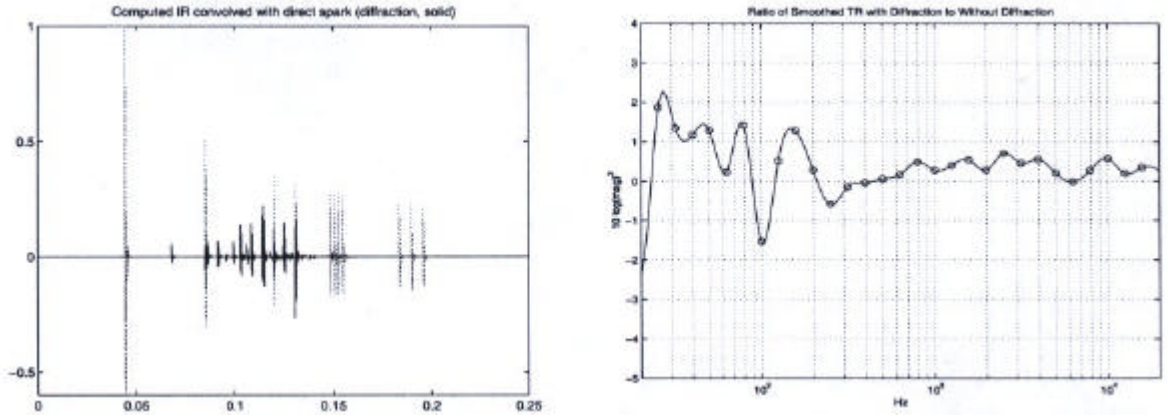

Figure 2. (a) The computed RIR (normalized and filtered with the measured spark source) with diffraction in solid lines, and specular reflections in dashed lines. (b) The level *difference* (maximum about 2 dB) “with and without” computed diffraction (all orders and combinations). The frequency curve is smoothed over third-octaves, where the horizontal axis is in Hz.

INPUT SIGNAL	*Are the diffraction contributions audible?*	*Is 2nd-order diffraction audible?*
Click	YES (18/18)	NO (6/18)
Organ	YES (13/18)	NO (10/18)
Noise	YES (13/18)	(not tested)
Female Voice	NO (9/18)	(not tested)
Male Voice	NO (7/18)	(not tested)

Table 1. ABX listening-test results with various orders and components of edge-diffraction. Second-order diffraction becomes more audible, however, in shadowed receiver positions.

Thus, although the total diffraction calculated in this conservative case may have seemingly small effects on numerical parameters (i.e., corresponding to spectral changes of 1-2 dB), they are nevertheless significant for auralization. Moreover, given the chosen geometry (with large and smooth walls) and the non-shadowed source-receiver orientation, one would expect even greater effects, shifted higher in frequency, from smaller-scale diffracting surfaces distributed throughout a concert hall (e.g., overhead reflectors or irregular wall and ceiling profiles).

Neglecting second-order diffraction for this source-receiver orientation has essentially no audible spectral effect, with a maximum difference of about 0.5 dB in frequency response curves. This is reflected clearly in the listening tests. Nevertheless, one should not automatically neglect second-order diffraction, as it can become more important, e.g., for lower frequencies and smaller surfaces, grazing angles, and shadowed receiver positions. Further listening tests (for a shadowed receiver under a balcony) showed that second-order edge diffraction was audible for all tested signals. More investigation is necessary in this area.

The listening test above was monaural, i.e., excludes head-related transfer functions (HRTFs). However, this still simulates the basic changes (due to including edge diffraction) in the early RIR for source-receiver orientations that involve predominantly frontal HRTF angles and are situated near the centerline, as in our case. Also, we propose below a practical implementation for binaural simulation of edge diffraction, based on its singular behavior along the least-time path for a given source-wedge-receiver orientation. Moreover, this initial study provides at least a first major step toward computing edge diffraction for room acoustics and auralization.

EDGE DIFFRACTION FROM REFLECTORS

In comparison to the stage house (where diffraction was a smaller, low-frequency effect in the presence of large, smooth reflecting surfaces), an array of smaller overhead rectangular reflectors forms a complementary study. First, one can examine a simpler impulse response (i.e., the direct sound, edge diffraction, and possibly a specular reflection) to gain clearer insight into diffraction effects. An advantage, moreover, of the time-domain formulation is that one may separate (or "dissect") the different transient components. (The stage-house impulse response was composed of many reflections whose individual effects were not distinguished.)

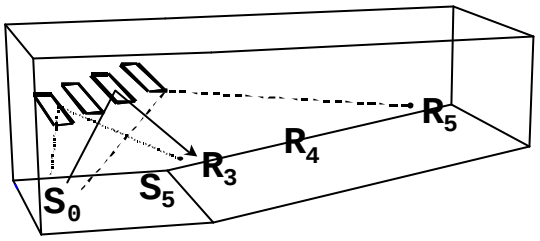

Figure 3. The reflector array. Source S5 is about 1 m from receiver R1 (not shown).

The modeled reflector array is shown in Figure 3, along with various source and receiver positions. We compute first- and second-order diffraction, including paths from one reflector to another. The computed impulse response from the reflector array for source-receiver S0-R3 is shown in Figure 4, where the different components are distinguished. Since the reflecting surfaces are much smaller than the stage-house walls, the resulting edge-diffraction interference should also affect higher frequencies, as we see in preliminary results below. The lower two (unsmoothed) frequency plots show level differences when diffraction is modeled. In the lower left plot (for S0-R5), edge-diffraction interference extends into the mid-frequency range. The greater influence of diffraction may be related to the grazing incidence angle to the receiver. For the lower right plot, source S5 and receiver R1 are about 1.4 m apart, directly under the highest reflector. Edge diffraction has less effect here, perhaps because the direct sound and specular reflection dominate. In any case, there appears to be a dependence on source-receiver orientation relative to the reflector array, and one can show that second-order diffraction cannot be neglected at lower frequencies.

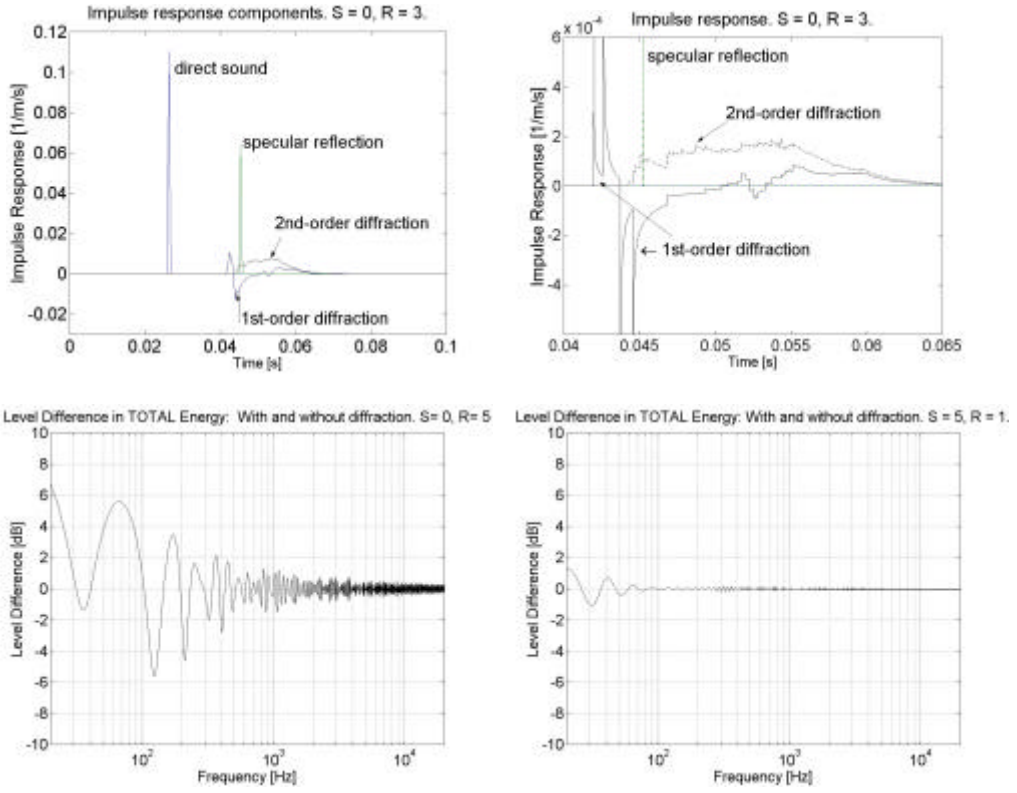

Figure 4. The top two plots show the computed impulse response for S0 and R3. Some of the diffraction components precede the specular reflection because the reflector array is stepped (i.e., does not lie within one plane). The right figure magnifies a high-resolution calculation. The lower frequency plots show level differences (some up to 6 dB) when diffraction is modeled for source-receiver S0-R5, and S5-R1. The direct sound (at 1.4-m distance) may dominate in the latter case.

COMPUTATIONAL CONSIDERATIONS

Edge Visibility Checks

As discussed above, the stage-house study required modeling of the following combinations of specular/diffracted components: *sp-ed*, *ed-sp*, and *sp-ed-sp*. For a simple barrier on a reflecting plane, these three paths are modeled with straightforward use of image sources and image receivers (e.g., Sec. 4 in [4]). For a room, however, with a multitude of reflection paths among concave and convex wedges, one must also construct physically sensible "visibility checks" of whether a given edge contributes diffraction for a selected source-receiver combination.

The *sp-ed* paths, for example, are modeled by replacing each first-order specular reflection with an image source for each reflecting plane. As shown in Fig. 5, however, the edge-visibility check must be able to determine that edge *E1* (perpendicular to the page) is visible to the image source *S¢* and that *E2* is not. Thus, the following visibility check is performed: (1) Check that the path from the image source to the first endpoint of an edge passes through the reflecting plane and is not blocked (e.g., by other planes). (2) Repeat for the second edge point. (3) If at least one of the two edge points is visible, assume that the edge is visible. In addition to this edge-visibility check, all edges of the reflecting plane must also be excluded. For example, although plane *F* is not "visible" (as it spawned the image source), plane *Q* and its edges may be visible via plane *F* for a different source position. The edge that plane *Q* shares with plane *F* may then be considered visible. Such errors must be avoided.

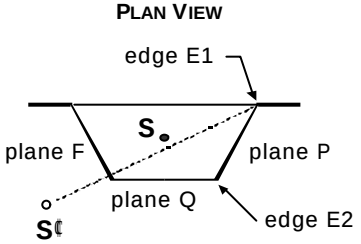

Figure 5. The edge-visibility check should determine that edge *E1* is visible and that *E2* is not.

This initial extension of the program does not divide edges into visible and hidden segments. Thus, Step 3 above is a choice between two approximations: to consider partially visible edges (1) as totally visible or (2) as totally hidden. The first approximation is selected because the visible part of the edge *still* diffracts, although with shortened edge length, whereas the second approximation entirely neglects this diffraction. Although our RIR measurements indicate that we have chosen the better approximation (or that the choice makes little difference here), future implementations of these calculations should further divide edges into visible and non-visible segments.

To summarize, after the visibility checks are completed, the following combinations of specular/diffractive components are computed:

$$h_{sp-ed}(t;S \mid R) = \sum_i \sum_j h_{diffr1}(t;S_i' \mid E_j \mid R)$$

$$h_{ed-sp}(t;S \mid R) = \sum_i \sum_j h_{diffr1}(t;S \mid E_j \mid R_i')$$

$$h_{sp-ed-sp}(t;S \mid R) = \sum_i \sum_j \sum_k h_{diffr1}(t;S_i' \mid E_j \mid R_k') .$$

In the first equation, for example, $h_{sp\text{-}ed}$ is the impulse response for the *sp-ed* paths between the source *S* and the receiver *R*, h_{diff1} represents first-order edge diffraction from an image

source S_i¢ via each visible edge E_j to the receiver R, and t is time. (An image receiver is denoted by R¢.)The summations are done over the indices that remain after the edge-visibility checks.

Binaural Simulation of Edge Diffraction

For binaural simulation, one must apply head-related transfer functions (HRTFs) to filter the edge-diffraction components. A brute-force assignment of several HRTFs for all of the edge sources along each wedge would be impractical and presumably subjectively unnecessary, as HRTF magnitude functions (as a rule of thumb) vary slowly over 5-10 degree increments [17]. We thus suggest a practical implementation for binaural simulation of edge diffraction, based on its singular behavior along the least-time path for a given source-wedge-receiver orientation.

As shown in Fig. 2 of Ref. 12, the "least-time" point (or "apex" point) A lies on the shortest path L_0 from the source S to the receiver R via the (infinite) wedge. The diffraction amplitude from this point is theoretically singular. This corresponds to a time t such that $\sinh[h(t)] = 0$ in the denominator of Eq. 1 in Ref. 12, after which the amplitude drops and then decays with time, initially by about $[\mathrm{sqrt}(t)]^{-1}$. Thus, the outer parts of the edge contribute significantly less to the diffraction, except possibly at very low frequencies. This is also evident in measurements and computations. With this in mind, one can use the least-time point on the wedge as a coordinate representing the entire edge relative to the listener, and with this approximation, each wedge then requires only one HRTF.

The source and receiver may also be oriented such that the least-time path for the actual finite wedge does not correspond to the least-time path for its ("virtual") infinite counterpart. In this case, the onset diffraction amplitude could be much less (as discussed with Fig. 2 of Ref. 7), but the "initial incidence point" (i.e., the endpoint that diffracts first to the receiver from the finite wedge) could still be used to determine the "equivalent" HRTF angle.

FUTURE WORK

Future work will include the modeling of more complex spaces and binaural implementation of edge diffraction and reverberation. Further comparison with measurements would allow insight into potential approximations to the numerical modeling, e.g., to possibly increase calculation speed or extend the model's applicability to finite impedance surfaces.

ACKNOWLEDGEMENTS

Financial support was provided by the Axel and Margaret Ax-son Johnsons Foundation, Sweden. The authors also appreciated discussions with consultants at Akustikon (Göteborg) and with Prof. M. Vorländer at ITA, RWTH-Aachen.

REFERENCES

[1] M. A. Biot and I. Tolstoy, *J. Acoust. Soc. Am.* 29, 381-391 (1957).
[2] J. P. Chambers and Y. H. Berthelot*, J. Acoust. Soc. Am*., 96, 1887-1892 (1994).
[3] G. M. Jebsen and H. Medwin, *J. Acoust. Soc. Am.* 72(5), 1607-1611 (1982).
[4] H.G. Jonasson, *J. Sound and Vib*. 22(1), 113-126 (1972).
[5] R. S. Keiffer *et al*. *J. Acoust. Soc. Am*., 95, 3-12 (1994).
[6] R. S. Keiffer *et al*., *Math. Modell. Sci. Comput*. 4, 414-419 (1994).
[7] R. S. Keiffer and J. C. Novarini, *J. Acoust. Soc. Am*., 107(1), pp. 27-39 (2000).
[8] P. S. Kovitz, Ph.D. thesis, Penn State University, Pennsylvania (1994).
[9] H. Medwin, *J. Acoust. Soc. Am.* 69, 1060-1064, (1981).
[10] H. Medwin *et al*. *J. Acoust. Soc. Am.* 72, 1005-1013 (1982).
[11] D. Ouis, *Appl. Acoust*. 56, 1-24 (1999).
[12] U. P. Svensson *et al*. *J. Acoust. Soc. Am*. 106, 2331-2344 (1999).
[13] R. R. Torres *et al*. "Audibility of 'diffusion' in room acoustics auralization: an initial investigation," *Acustica* (in press 2000).
[14] R. R. Torres and M. Kleiner, *Proc. of the 16th ICA and 135th ASA*, 371-372 (1998).
[15] R. R. Torres, U. P. Svensson, M. Kleiner. "Computation of edge diffraction for room acoustics auralization" (submitted).
[16] G.Wadsworth and J. P. Chambers, *J. Acoust. Soc. Am*.107, 2344-2350 (2000).

[17] D. Begault and E. Wenzel, personal communication.